Consequence of the Removal of Evolutionary Conserved Disulfide Bridges on the Structure and Function of Charybdotoxin and Evidence That Particular Cysteine Spacings Govern Specific Disulfide Bond Formation

Eugenia Drakopoulou,[‡] Jean Vizzavona,[‡] Jacques Neyton,[§] Vincent Aniort,[‡] Françoise Bouet,[‡] Henri Virelizier,[∥] André Ménez,[‡] and Claudio Vita*,[‡]

CEA, Département d'Ingénierie et d'Etudes des Protéines, Service de Physique d'Expérimentation et d'Analyse, Saclay, 91190 Gif-sur-Yvette, France and Laboratoire de Neurobiologie, Ecole Normale Superieure, 75230 Paris, France

Received August 25, 1997; Revised Manuscript Received November 14, 1997

ABSTRACT: Scorpion toxins are miniglobular proteins containing a common structural motif formed by an α-helix on one face, an antiparallel *β*-sheet on the opposite face, and three disulfide bonds making up most of its internal volume. We have investigated the role of these evolutionary conserved bonds by replacing each couple of bridged cysteine residues of the scorpion charybdotoxin by a pair of nonbridging L-α-aminobutyric acid (Aba) residues. Three analogues were obtained by solid-phase synthesis, Chab I, Chab II, and Chab III, containing the Aba residues in positions 7 and 28, 13 and 33, 17 and 35, respectively. Circular dichroism analysis showed that the purified Chab II acquired a conformation similar to that of charybdotoxin, while the Chab I and Chab III possess decreased nativelike characteristics. All analogues block single high-conductance Ca^{2+}-activated K^+ channels from rat skeletal muscle inserted into planar lipid bilayers, but with different potencies. Chab II is the most active analogue ($K_D = 8.0 \times 10^{-8}$ M), with a 9-fold lower affinity as compared to native charybdotoxin. Chab I and Chab III have, respectively, 180- and 580-fold lower affinity. Therefore, the removal of evolutionary conserved disulfide bridges does not prevent the toxin to adopt a functional and presumably nativelike structure. However, removal of one disulfide bond affects the yields of formation of correct pairing between the remaining cysteine residues, and only Chab I preserves the ability to form the native disulfide pairings with high efficiency. This is the only analogue to preserve particular spacings of three and one residue between the cysteines, which have been described to thermodynamically disfavor disulfide bond formation between the cysteines [Zhang, R., and Snyder, G. H. (1989) *J. Biol. Chem. 264*, 18472−18479]. Therefore, we conclude that the position of the cysteine residues in the sequence of charybdotoxin, by disfavoring specific pairings and favoring others, may govern selective formation of specific disulfide bonds, thus, explaining the efficient folding properties of Chab I and of native charybdotoxin. The structural properties of the Chab analogues and the discovered role of the cysteine spacings have interesting implications in protein design and engineering.

Charybdotoxin (Chtx),[1] a 37-residue protein toxin found in the Israeli *Leiurus quinquestriatus* scorpion venom (*1, 2*) is a powerful inhibitor of many types of K^+-selective ion channel, from the two major classes of voltage-gated and Ca^{2+}- activated channels (*3*−*9*). This and other scorpion toxins have become valuable tools for the investigation of the K^+ channels, in particular, to identify the organization of channel pore-forming region (*5, 10*) and as a caliper to estimate the dimension of the outer pore mouth of K^+ channels (*11*−*17*). These toxins have also found useful applications in the determination of the subunit stoichiometry of voltage-gated K^+ channels (*18, 19*) and in the localization and tissue distribution of individual channel subtypes (*20, 21*).

Charybdotoxin, together with the other K^+ channel inhibitors present in scorpion venoms, form a family of structurally related small proteins. The three-dimensional structure of many of them has been solved in aqueous solution by multidimensional-NMR (*22*−*28*). All of them present the same α/*β* fold which consists of an α-helix linked to an antiparallel triple stranded *β*-sheet by two disulfides; a third disulfide links the *β*-sheet to an extended segment preceding the helix (Figure 1). The three disulfides make up most of the internal volume. Strikingly, the same α/*β* structural motif was found to be present in longer scorpion toxins (60−65 residues), which act on Na^+ channels (*22, 23*), in insect defensins, which are produced in response to bacterial

* To whom correspondence and reprint requests should be addressed. Tel: 33 1 69087133. Fax: 33 1 69089137.

[‡] Départment d'Ingénierie et d'Etudes des Proteines.

[§] Laboratoire de Neurobiologie.

[∥] Service de Physique, d'Expérimentation et d'Analyse.

[1] Abbreviations: Aba, L-α-aminobutyric acid; Chtx, charybdotoxin; Chab I, ([Aba^{7,28}]charybdotoxin); Chab II, ([Aba^{13,33}]charybdotoxin); Chab III ([Aba^{17,35}]charybdotoxin; CD, circular dichroism; 2D, two-dimensional; ES-MS, electrospray mass spectrometry; Fmoc, 9-fluorenylmethoxycarbonyl; GSH, reduced glutathione; GSSG, oxidized glutathione; HBTU, [2-(1-*H*-benzotriazol-1-yl]-1,1,3,3-tetramethyluronium hexafluorophosphate; HOBt, 1-hydroxybenzotriazole; HPLC, high performance liquid chromatography; NMR, nuclear magnetic resonance.

S0006-2960(97)02108-9 CCC: $15.00
Published on Web 01/15/1998

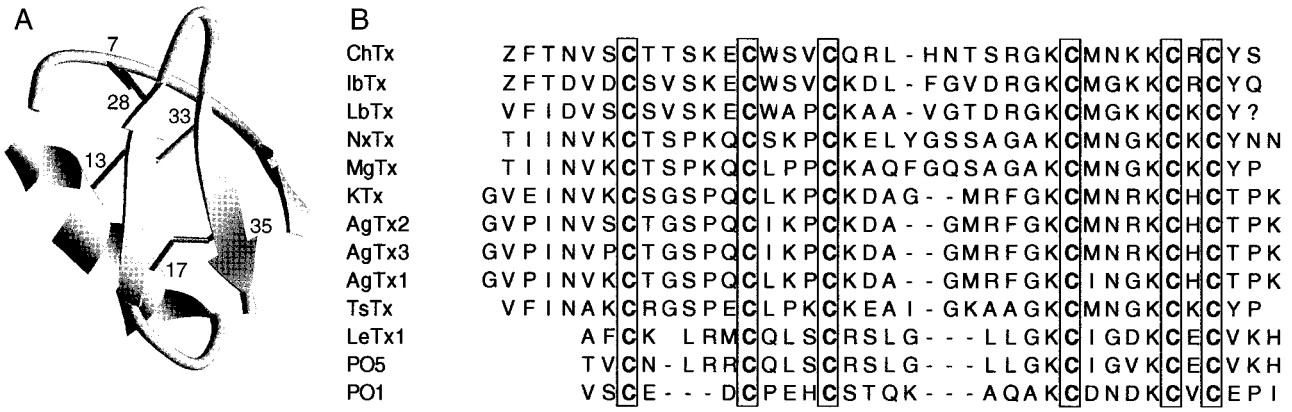

FIGURE 1: (A) Three-dimensional structure of charybdotoxin (PDB code, 2CRD). Numbers indicate the position of cysteine residues. (B) Sequence alignment of short scorpion toxins. Abbreviations to common names are ChTx, charybdotoxin (*2*); IbTx, iberiotoxin (*69*); LbTx, limbatustoxin (*70*); NxTx, noxiustoxin (*71*); MgTx, margatoxin (*70*); KTx, kaliotoxin (*72*); AgTx2, AgTx3, AgTx1, agitoxin 2, 3, 1 (*73*); TsTx, tityustoxin-Kα (*74*); LeTx 1, leiurotoxin 1 (scyllatoxin) (*75*); P05 (*76*); P01 (*77*). Z is 5-oxoproline (pyroglutamic acid).

infection (*29*), and also in plant γ-thionins (*30*). Thus, this simple and well-ordered structural motif has not only been used by scorpions to develop biological activities (blockage of K^+ and Na^+ channels) in order to subdue prey, but also by different animals to defend themselves against bacterial attack, thus, emphasizing the great functional versatility of this fold. Interestingly, an alignment of the sequences of short scorpion toxins (Figure 1B) reveals that the only conserved residues are the six cysteines involved in the three disulfide bonds and that there is a conserved spacing of three residues between the two cysteines located on the helix and one residue between the two cysteines of the β-sheet (*23*): this spacing was indicated as the sequence determinant of the structural conservation of two disulfide bonds linking the helix to the β-sheet and takes part of the sequence consensus motif, C...CxxxC...C...CxC (where x is any amino acid residue) characteristic of the α/β scorpion fold (*23*).

The high sequence permissiveness and functional versatility make the α/β fold of scorpion toxins a particularly attractive scaffold for protein engineering. Thus, we use it as a structural host scaffold and transferred structurally compatible active sequences on its β-sheet, leading to novel chimeric miniproteins with new unrelated activities, including metal binding property (*31*) and nicotinic acetylcholine receptor binding activity (*32, 33*). Since the cysteine residues are buried inside the molecule and are conserved in all scorpion toxins, we maintained the cysteine position in the engineering of new sequences and mutated only the solvent exposed residues. As demonstrated by ^{1}H NMR analysis (*31, 33*), the two novel miniproteins preserved the α/β fold of scorpion toxins, the network of disulfide bonds, the internal interactions, and a rapid folding ability, which gave a unique and native set of cysteine bonding, like the natural sequence.

Although the disulfide bonds in natural scorpion toxins and in the newly engineered sequences are important in maintaining the active three-dimensional structure, how these disulfides are able to form and to contribute to the native fold is unknown. Studies on other disulfide-containing proteins, including bovine trypsin inhibitor (BPTI) (*34*−*36*), ribonuclease A (*37*−*39*), ribonuclease T1 (*40*) have demonstrated that the formation of distinct disulfide bonds is regulated by weak noncovalent interactions favoring specific positioning of the cysteine thiols that lead to the formation of disulfide bonds. However, in small proteins containing multiple disulfides, like in conotoxins (13 residues) (*41*−*43*), in apamin and sarafotoxin (18−21 residues) (*44*), the number of residues intervening between the half-cystines has been proposed to be a determining factor in governing selective formation of specific disulfides.

As a part of a study aimed to investigate relationships that may link the active three-dimensional structure of the scorpion fold to a specific positioning of half-cystines and arrangement of disulfide bonds, we replaced, chemically, each individual half-cystine of charybdotoxin by a pair of L-α-aminobutyric acid (Aba) residues. This amino acid is isosteric to half-cystine and has a similar polarity (*45, 46*); therefore, it is considered to be more suitable for replacing bridged cysteines than Ser and Ala residues. Three analogues, possessing only two native disulfide bridges and two Abas, were thus synthesized, Chab I ([Aba^{7,27}]charybdotoxin), Chab II ([Aba^{13,33}]charybdotoxin), and Chab III ([Aba^{17,35}]-charybdotoxin). In this paper, we report the synthesis and structural and functional characterization of these analogues. Our results show that the effects on structure and function depend on the positions of the cysteine residues that are substituted. Furthermore, analysis of the isomers formed in the oxidative folding process of the three analogues indicates that the conserved cysteine spacings of three and one residues intervening between two cysteines determine specific native disulfide arrangements, thus, explaining the efficient folding properties of both charybdotoxin and its engineered sequences.

MATERIALS AND METHODS

Materials. Fluorenylmethyloxycarbonyl (Fmoc) amino acid derivatives were purchased from Nova Biochem. The solvents *N*-methylpyrollidone, dimethylformamide, 2-propanol, methyl-*tert*-butyl ether, and acetonitrile, as well as the reagents acetic acid, trifluoroacetic acid, diisopropylethylamine, and piperidine, were from SDS (Peypin, France). Thioanisole, ethanedithiol, phenol, and acetic anhydride were from Fluka. The 1-hydroxybenzotriazole (HOBt), [2-(1-*H*-benzotriazol-1-yl]-1,1,3,3-tetramethyluronium hexafluorophosphate (HBTU) and the ninhydrin reagents were from Applied Biosystems (Paris, France). Reduced, oxidized

glutathione, trypsin, Tris, and HEPES buffer were from Sigma (St. Louis, MO). Charybdotoxin was synthesized as described (*47*, *48*). Sequanal grade guanidine hydrochloride were from Pierce. The lipids, used in biological activity tests, were 1-palmitoyl, 2-oleoyl phosphatidylethanolamine (POPE) and the analogous phosphatidylcholine (POPC), obtained from Avanti Polar Lipids, Inc. (Birmingham, AL) and stored as stock solutions in chloroform under nitrogen at −70 °C. Plasma membrane vesicles were prepared from rat skeletal muscle as described (*49*) and stored in 0.4 M sucrose at −70 °C. All inorganic salts were of analysis grade and obtained from Prolabo (Paris, France).

Synthesis. Synthesis was carried out on a Applied Biosystems 430A peptide synthesizer, using Fmoc/*tert*-butyl strategy and HBTU/HOBt coupling (*50*). Amino acid side chain blocking groups were *tert*-butyl ether for Ser and Thr; *tert*-butyl ester for Asp and Glu; 2,2,5,7,8-pentamethylchromane-6-sulfonyl for Arg; trityl for Asn, Cys, His, and Gln; and *tert*-butyloxycarbonyl for Lys. Pyroglutamic acid (5-oxoproline) was used without protection. The C-terminal amino acid Fmoc-Ser(*tert*-butyl)-OH was manually coupled (*51*) to the hydroxymethylphenoxy polystyrene resin (HMP-resin, Applied Biosystems) to obtain a final substitution of 0.5 mmol/g. Peptide synthesis was accomplished on a 0.25 mmol scale. Single 30 min coupling with 4-fold Fmoc-amino acid excess was used (only sequence 16−20 was double coupled), followed by capping with acetic anhydride. Coupling efficiency of each step of the entire synthesis was measured by quantitative ninhydrin method (*52*). The average coupling yield for final amino acid incorporation was 99.6% for Chab I, 99.4% for Chab II, and 99.3% for Chab III. The peptide was cleaved from the solid support with simultaneous removal of side-chain protective groups by treatment with reagent K (82.5% trifluoroacetic acid, 5% water, 5% phenol, 5% thioanisole, and 2.5% ethanedithiol) for 1.5 h at room temperature (*53*). The resin was filtered, and the free peptide was precipitated in methyl-*tert*-butyl ether at 4 °C. After centrifugation and washing three times with ether, the peptide was dissolved in 20% acetic acid and lyophilized. The crude lyophilized product was desalted by gel-filtration on a Sephadex G25M column (4 × 40 cm), eluted with 10% acetic acid, and lyophilized. The crude reduced peptides were obtained in overall yields corresponding to 80% for Chab I, 71% for Chab II, and 74% for Chab III.

Folding and Purification. Lyophilized reduced product was dissolved (5 mg/mL) in water and added (0.1 mg/mL, final concentration of protein) to the oxidizing buffer, consisting of 0.05 M sodium phosphate, 0.2 M NaCl, 5 mM oxidized glutathione, and 0.5 mM reduced glutathione, pH 7.8. After 2 h at room temperature, the oxidation solution was acidified to pH 3.0 with acetic acid and loaded directly on a C_8 Aquapore RP300 column (1 × 25 cm) at 2 mL/min flow rate. The oxidized protein was then eluted using a linear gradient of 15 to 35% acetonitrile in 0.1% aqueous trifluoroacetic acid over 30 min at 6 mL/min flow rate. Fractions containing the correctly folded protein were further purified on a Vydac C_{18} column (1 × 25 cm) eluted at 5 mL/min with a 40 min linear 15 to 25% acetonitrile gradient in 0.1% aqueous trifluoroacetic acid.

Amino Acid Analysis and Sequence Determination. Samples of pure lyophilized product (0.1−1 nmol) were hydrolyzed under vacuum with 6 N HCl at 120 °C for 17 h. The free amino acids were converted into phenylthiocarbamoyl (PTC) derivatives and analyzed on an Applied Biosystems 130A automatic analyzer. Phenylthiocarbamoyl-Aba was eluted between the proline and tyrosine derivatives. Sequence determination was automatically performed on an Applied Biosystems 477A protein sequencer. Phenylthiohydantoin-Aba derivative was eluted between the tyrosine and proline derivatives.

Mass Analysis. Ion electrospray mass spectra were determined on a Nermag R10-10 mass spectrometer, coupled to an Analytica of Brandford electrospray source. The quadrupole was scanning over the range *m*/*z* 300−2000. A HP-ChemStation software (Hewlett-Packard) was used to drive the spectrometer and to acquire the data.

Peptide Mapping. The oxidized Chtx and the three Chab proteins (50 μg) were digested with trypsin (10 μg) in a buffer containing 0.1 M Tris·HCl and 4 mM $CaCl_2$, pH 8.0, at 37 °C for 15 h. Then, 100 μL of 10% trifluoroacetic acid was added to stop the reaction, and the digest was loaded on a Vydac C_{18} column (0.46 × 25 cm) using a linear gradient of 1 to 25% acetonitrile over 45 min or 0 to 40% over 40 min, at a flow rate of 0.75 mL/min. Peaks were collected, lyophilized, and identified by amino acid and sequence analysis or by mass determination.

Circular Dichroism. Circular dichroism spectra were recorded on a Jobin Yvon CD6 dichrograph, equipped with a thermostatically controlled cell holder and a IBM-PC operating with a CD6 data acquisition and manipulation program. Spectra were recorded at 20 °C in 10 mM phosphate buffer, pH 7.5, by accumulating 4 scans obtained with an integration time of 0.5 s every 0.2 nm. In the far-UV region (180−250 nm) the protein sample was at (2−2.5) × 10^{-5}M in a 0.1 cm path length quartz cell; in the near UV region (250−320 nm), the protein sample was at (2−2.5) × 10^{-4} M in a 1 cm path length quartz cell.

Biological Activity. The channel blocking activities of the different toxin variants were quantified on single high-conductance Ca^{2+}-activated channels from rat skeletal muscle inserted into planar lipid bilayers. Channels were inserted into the lipid bilayer as described previously (*54*) by fusion of plasma membrane vesicles with painted bilayers made with a mixture of POPE and POPC (ratio 7:3) solubilized at 20 mg/mL in *n*-decane. The fusion process was promoted by the presence of a transmembrane osmotic gradient which could be rapidly removed allowing the insertion of a single channel. The orientation of the channel insertion was determined from the polarity of the channel voltage dependence. After channel insertion, the inner ("cytoplasmic") and external ("extracellular") compartments were washed with solutions containing, in millimolarity, 150 KCl and 10 HEPES (pH adjusted to 7.4 with KOH) and 150 NaCl, 1 KCl, and 10 HEPES (pH adjusted to 7.4 with KOH), respectively. A high level of activation of the channel under study (open probability above 0.95) was obtained by systematically adding $CaCl_2$ (0.5 mM) and $MgCl_2$ (5 mM) to the inner compartment (*55*). The transmembrane voltage was maintained constantly at +30 mV (the electrophysiological voltage convention is always used here, with the external side of the channel defined as zero voltage). All experiments were performed at room temperature (20−23 °C). The electronics of the voltage-clamp system followed

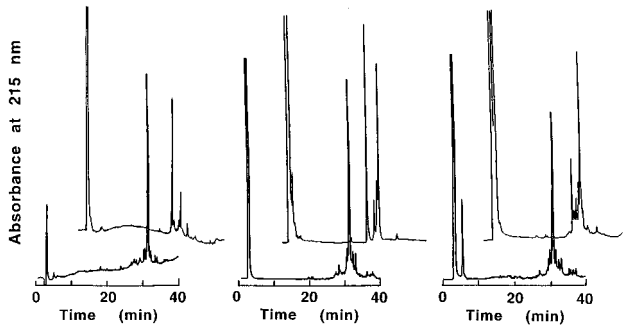

FIGURE 2: Analytical reverse-phase HPLC profiles of the crude reduced (lower traces) and oxidized (upper traces) Chab I (left), Chab II (center), and Chab III (right). A Vydac C18 column (0.46 × 15 cm) was used, equilibrated with 0.1% trifluoroacetic acid and eluted with a linear 5 to 40% acetonitrile gradient over 40 min at a 1 mL/min flowrate. Detection was at 215 nm.

the design of Hanke and Miller (*56*). The current signal was filtered at 500 Hz and then collected at a sampling interval of 0.5 ms by a MINC 1123 computer (Digital Equipment Corp., Marlboro, MA). The association and dissociation kinetics of each toxin variant were measured from the statistical distribution of at least 100 discrete blocking events, which were induced by the addition of peptide to the external compartment. In our recording conditions, blocking events, defined as shut periods longer than a cutoff time of 200 ms, were easily distinguished from the channel gating activity (mean closed time < 5 ms). The mean durations of the blocked events (t_{bl}) and of the bursts (t_{bu}) separating successive blocked events were calculated using regular corrections for missed events (*57*) and used to estimate the apparent rates of dissociation and association of the toxin variants. Charybdotoxin is known to interact with the channel with a bimolecular reaction mechanism (*58*). Assuming a similar mechanism for the Chab analogues, we have $k_{on} = t_{bu}^{-1}[\text{toxin}]^{-1}$, and $k_{off} = 1/t_{bl}$.

Folding Studies. Pure reduced analogues were obtained from purified oxidized products by 30 min treatment with 0.1 M dithiothreitol (DTT) in 8.0 M guanidine·HCl and 0.1 M Tris·HCl, pH 8.0, followed by purification on reverse phase HPLC and lyophilization. Folding experiments were performed by diluting the reduced analogues solutions [$(2-4) \times 10^{-4}$ M in degassed water, pH 3.0] to the final protein concentration of 1.5×10^{-5} M into degassed and argon conditioned solutions of 0.1 M Tris·HCl, 0.2 M NaCl, 1 mM EDTA, 5 mM oxidized glutathione, and 0.5 mM reduced glutathione, pH 7.8, in the absence or in the presence of different concentrations of guanidine·HCl. Reaction was stopped after 60 min by acetic acid addition and solutions were injected into a Vydac C18 (0.46 × 25 cm) column, eluted with a 30 min linear gradient of 5 to 40% acetonitrile in 0.1% aqueous trifluoroacetic acid. Eluted peaks were collected, lyophilized, and analyzed by ES-MS.

RESULTS

Synthesis, Purification, and Disulfide Bond Assignment. The three synthetic charybdotoxin analogues missing one disulfide, Chab I, Chab II, and Chab III, were analyzed by reverse-phase HPLC and shown to present a major peak (Figure 2). The quality of the crude peptides was considered to be satisfactory to proceed to disulfide formation without previous purification. Oxidation of charybdotoxin analogues was tested in the presence of different ratios of oxidized (GSSG)/reduced (GSH) glutathione. The GSSG/GSH ratio corresponding to 5/0.5 mM gave the highest yields in disulfide formation. We anticipated that the correctly folded species may elute earlier in reverse-phase HPLC (*47*), since the molecule presenting the native disulfides is expected to best bury the nonpolar group in the interior of the molecule protected from interactions with the hydrophobic column packings and solvent (*44*, *59*). As shown in Figure 2, for all three charybdotoxin analogues, Chab I, Chab II, and Chab III, a single peak eluted earlier, at 25−26 min, separated from other species. However, even if the crude synthetic materials were of similar homogeneity, the area of the earlier eluted peaks represented a different proportion of the total eluting material, accounting to ∼80% for Chab I, ∼38% for Chab II, and ∼15% for Chab III, suggesting quite different yields in correct disulfide formation in the three synthetic analogues (vide infra). The material contained in the earlier eluted peaks was purified to homogeneity by semipreparative reverse-phase HPLC. Amino acid composition of the purified analogues agreed with the expected ones. Electrospray mass spectrometry of the purified products gave experimental M_r of 4261.9 Da for Chab I, 4261.9 Da for Chab II, and 4261.4 Da for Chab III. These values are in good agreement with the theoretical M_r of 4261.7 Da and confirm the presence of two disulfide bonds. For each Chab molecule purified, the cysteine pairing was examined by tryptic mapping. The fragments, obtained after trypsin digestion, were separated by reverse-phase HPLC and identified by amino acid analysis and sequencing, as already described (*47*). The results of this analysis (Table 1 in Supporting Information) indicate that all the three isolated and purified species, earlier eluted in reverse-phase HPLC, contain the two remaining nativelike disulfide bonds: i.e., Chab I contains the disulfides 13−33 and 17−35, Chab II the disulfides 7−28 and 17−35, and Chab III the disulfides 7−28 and 13−33.

Biological Activity. The three Chab analogues have been tested for their ability to block high conductance Ca^{2+}-activated K^+ channels from rat skeletal muscle, which were inserted into planar lipid bilayers. Under conditions promoting a high channel activation level (see Materials and Methods), all three Chab analogues induced long shut events (duration > 200 ms), which were not present in control recordings (Figure 3). However, the mean duration of these blocking events differed from one Chab analogue to another. Native charybdotoxin induced blocks lasting for a few tens of seconds, whereas they were shorter (in the 5−10 s time scale) for Chab II, shorter again (0.5−2 s) for Chab I, and even shorter for Chab III (hundreds of milliseconds). From series of at least three independent measurements for each toxin analogue, apparent association and dissociation rates and the resulting dissociation constants were estimated for each variant (Table 1). The blocking potency of the Chab analogues compared with that of native charybdotoxin and the Chab analogues decreased in the following order: Chab II (9-fold) > Chab I (180-fold) > Chab III (580-fold). These differences mainly result from an increased dissociation rate in the case of Chab II, whereas both an increase in the dissociation rate and a decrease in the association rate are involved in the cases of Chab I and Chab III.

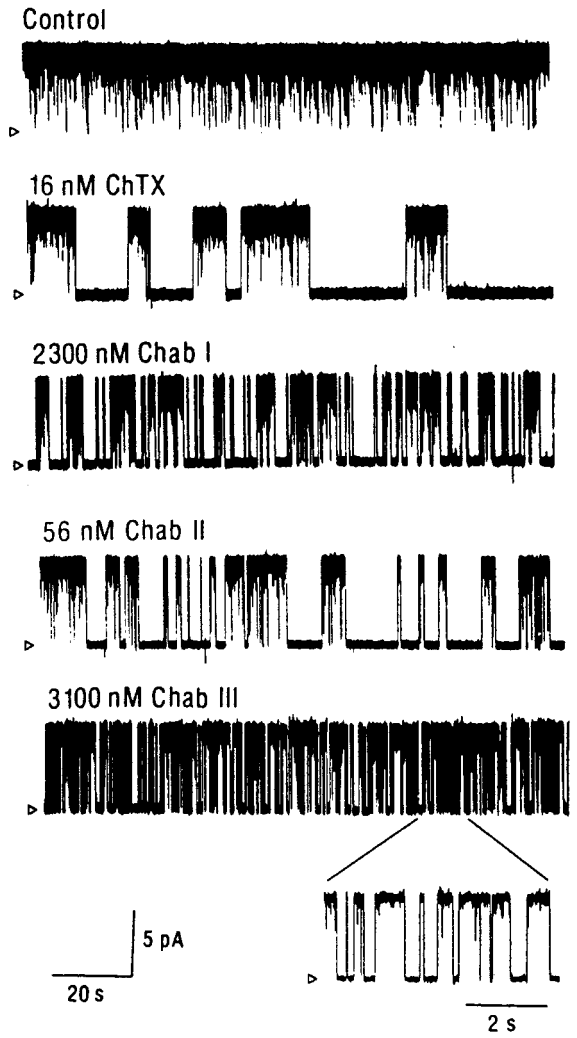

FIGURE 3: Blockade of Ca^{2+}-activated K^+ channels by native charybdotoxin (Chtx) and by the different Chab analogues. Single K^+ channels were inserted in lipid bilayers and recordings were obtained either in the absence of toxin (control) or in the presence of one of the different toxin variants added at the indicated concentration in the external compartment. In these recordings, channel openings are upward and the amplitude level of the closed or blocked states is indicated by open arrowheads. A portion of the recording obtained in the presence of Chab III is shown with a higher time scale to allow for resolution of the discrete blocking events. Holding potential, +30 mV.

Table 1: Kinetic Parameters of Blockade of K^+ Channel by Charybdotoxin, Chab I, Chab II, and Chab III

	k_{off} ($\times 10^2$ s)	k_{on} ($\times 10^{-6}$ M^{-1} s^{-1})	K_D (nM)	n
charybdotoxin	4.7 ± 0.9	5.7 ± 1.3	8.5 ± 2.3	5
Chab I	75 ± 10	0.49 ± 0.04	1500 ± 300	3
Chab II	26 ± 3	3.7 ± 1.3	80 ± 30	6
Chab III	290 ± 60	0.58 ± 0.04	4900 ± 700	3

[a] Each value represents the mean ±SD of n indepedent determinations of single channels, each recorded in a separate bilayer held at +30 mV.

Conformational Analysis. A CD analysis was performed for each Chab analogue and for native charybdotoxin in 10 mM phosphate buffer, pH 7.5. As seen in Figure 4, the far-UV spectrum of Chab II is similar to that of charybdotoxin, with a minimum at about 217 nm and a maximum at 194 nm; this maximun, however, is reduced in intensity and the CD spectrum crosses the *x*-axis at a lower wavelength as

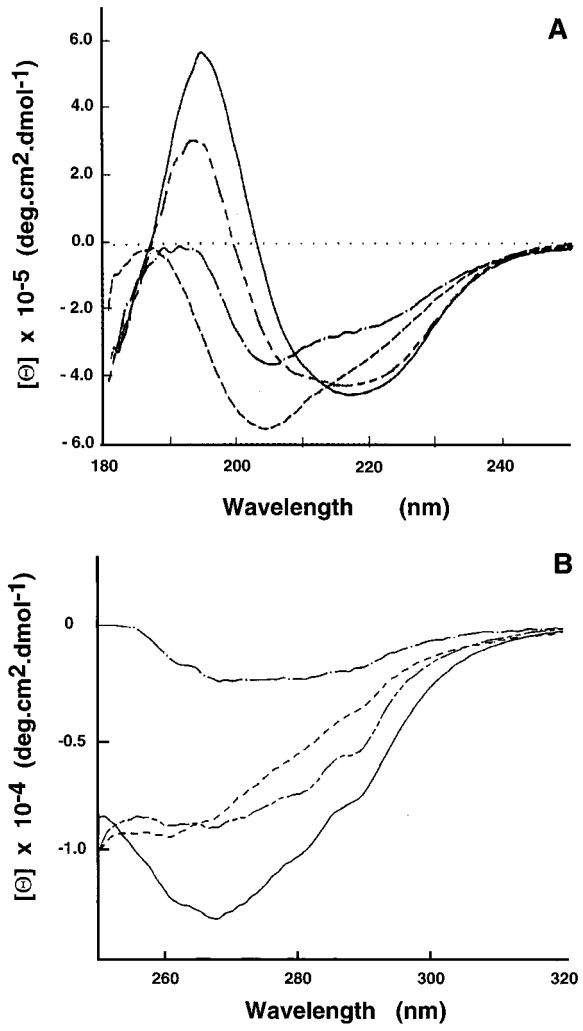

FIGURE 4: Circular dichroism spectra of charybdotoxin (—), Chab I (- - -), Chab II (— - - —) and Chab III (— - —) in the far-UV (A) and near-UV (B) region. Spectra were recordered at 20 °C in 10 mM phosphate buffer, pH 7.2. [Θ] is molar ellipticity.

compared to charybdotoxin. In the same region, Chab I and Chab III show significantly different CD spectra, with a minimum at 205 nm, a shoulder at 220 nm, and an ill-defined maximum around 190 nm. In the near-UV region (Figure 4B), charybdotoxin shows a CD spectrum indicative of the presence of both disulfide bridges (large negative band in the 250−300 nm range) and the aromatic amino acids, namely Phe2 (band at 262 and 268 nm), Trp14 (shoulder at 290 nm), and Tyr 36 (shoulder at 276 and 282 nm) (*47*). The same features are also present in the CD spectrum of Chab II, but are less visible in Chab I and even less in Chab III; notably, the contribution of tyrosine seems to be absent in Chab I and Chab III.

Effect of the Removal of a Disulfide Bond on Folding. To better understand the effect of the removal of one disulfide bond on cysteine pairing, we analyzed the oxidative folding process of the three analogues by reverse phase-HPLC and ES-MS, starting with purified reduced species. As shown in Figure 5 (top panels), when the reduced purified analogues are folded in the presence of excess of oxidized glutathione (5mM GSSG/0.5 mM GSH, pH 7.8), the HPLC profiles are essentially identical with those shown in Figure 2 and obtained by oxidation of the crude and reduced synthetic materials. This confirms that the different yields

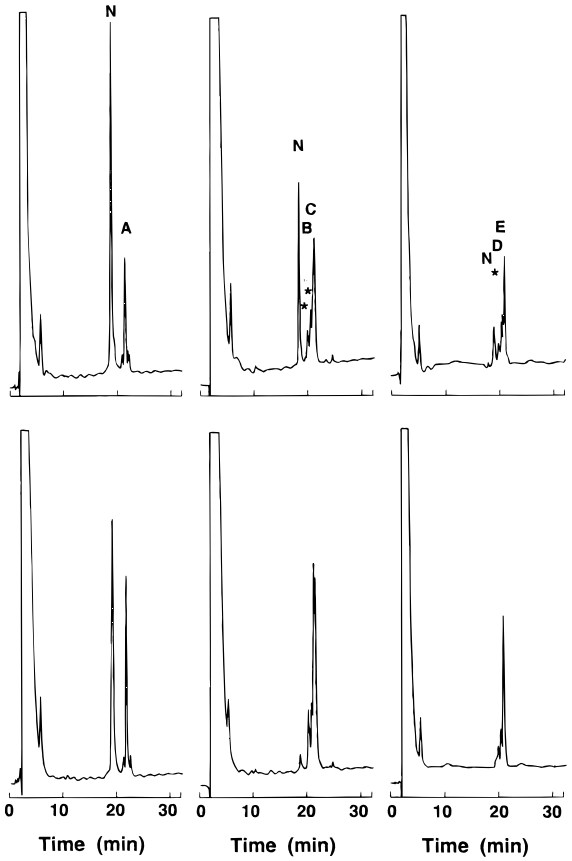

FIGURE 5: Reverse-phase HPLC profiles of the oxidation products of Chab I (left), Chab II (center), and Chab III (right) in the absence (top) and in the presence (bottom) of 6 M guanidine·HCl. N is the native form, A, B, C, D, and E are nonnative two-disulfide isomers. Asterisks indicate isomers containing glutathione-mixed disulfides. A Vydac C18 column (0.46 × 15 cm) was used, equilibrated with 0.1% trifluoroacetic acid and eluted with a linear 5 to 40% acetonitrile gradient over 30 min at a 1 mL/min flowrate. Detection was at 215 nm.

in the formation of the correctly folded analogues do not result from synthetic difficulties, but are presumably the consequences of the removal of two half-cystines. All the species formed and eluted from the HPLC column have been collected and their mass determined by ES-MS. This analysis reveals that Chab I, elutes at 18.7 min (species N, M_r = 4261.6 Da, Figure 5 top left), forms in high yields, and in addition *only another* isomer, the species A (eluted at 21.3 min) presenting the mass of 4261.3 Da is formed. In the Chab II oxidative folding, besides the Chab II itself (species N, eluted at 18.6 min in Figure 5, top center), four additional distinct molecular species are formed: species B (M_r = 4261.3 Da) and species C (M_r = 4261.4 Da), representing two isomers of Chab II with two different intrachain disulfides and two additional species (M_r = 4874.5 Da and M_r = 4874.6 Da) indicated by asterisks in the Figure 5, representing molecules containing one intrachain disulfide and two mixed disulfides with glutathione (M_r of glutathione = 612.6 Da). In the Chab III oxidative folding process (Figure 5, top right), Chab III (species N, eluted at 18.7 min; M_r = 4261.5 Da) is formed with low yields and three additional species are formed: species D (M_r = 4261.3 Da) and species E (M_r = 4261.4 Da), representing two isomers of Chab III, containing two different intrachain disulfides, and the species with an asterisk (M_r = 4874.5 Da), which contains one intrachain disulfide and two mixed disulfide with glutathione.

Table 2: Assignment of the Disulfide Bonds of the Chab I Isomers

peak (retention time)[a] (min)	molecular mass[b] (Da)	sequence	cysteine pairing
	Chab I (Isomer N)		
X2 (12.6)	476.0	28−31	
T1 (13.7)	726.3	20−25	
T2 (16.2)	960.2	15−19/35−37	C17−C35
T3 (22.2)	711.1	12−14/33−34	C13−C33
X1 (22.9)	1179.5	1−11	
	Chab I (Isomer A)		
X2 (12.8)	476.0	28−31	
T1 (14.0)	726.3	20−25	
T2′ (14.3)	866.2	15−19/33−34	C17−C33
X1 (23.0)	1179.5	1−11	
T3′ (24.6)	805.1	12−14/35−37	C13−C35

[a] Retention time on a Vydac C18 column (0.46 × 25 cm) eluted with a 40 min linear gradient 0 to 40% acetonitrile in 0.1% trifluoroacetic acid at 0.75 mL/min flow rate. [b] Determined by ES-MS.

To examine the sensitivity of the three Chab molecules to denaturing conditions, the folding studies have been repeated in the presence of 6 M guanidine·HCl. As shown in Figure 5 (bottom right), in denaturing conditions, the native Chab I isomer N still forms, but the nonnative isomer A is now increased in intensity. Both isomers formed in these conditions have been isolated, purified, submitted to trypsin hydrolysis and the fragments obtained analyzed by ES-MS. The results of this analysis are shown in Table 2: the isomer N contains the native disulfide bonds 17−35 and 13−33, as expected, while the isomer A contains the nonnative disulfide bonds 13−35 and 17−33. No species, containing the third possible disulfide pairing 13−17 and 33−35 has been detected. In contrast with the Chab I behavior, both the Chab II (Figure 5, bottom center) and Chab III (Figure 5, bottom right) sequences are sensitive to the presence of 6 M denaturant. The correctly folded molecules do not form any more; only the nonnative, lately eluted species are now present.

DISCUSSION

Functional Analysis and Correlation with Structure. By systematic mutagenesis experiments, the entire molecular surface of charybdotoxin, making direct contact with the K^+ channel, has been mapped (*12*, *60*, *61*). These studies show that the toxin interaction surface is formed by eight residues that project their side chains off the second and third strand of the β-sheet (Figure 1A), while, on the opposite side of the molecule, most residues of the helix project away from the interaction surface. Thus, the ability of the three Chab analogues to interact with the channel should strongly depend on the structure of the β-sheet molecular surface and on the ability of the analogue structure to present the functional groups of that region in a proper conformation. When tested on the K^+ channel, Chab II shows an affinity which is only 9-fold reduced, as compared to that of the native toxin (Table 1). Thus, the absence of the disulfide 13−33 in Chab II does not seem to affect notably the toxin affinity for the channel. The three-dimensional structure of Chab II has been recently solved in solution by 2D-NMR (*62*). From that study, it is evident that Chab II possesses a well-defined structure, which is very similar to that of native charybdot-

oxin, as judged from the low value (1.44 Å) of the averaged rms deviation between the backbone atoms of the best ten Chab II and charybdotoxin structures. In particular, the internal hydrophobic core of the molecule is the better defined region: doubtless, the hydrophobic nature of the Aba side chain positively contributes to the internal interactions and to form a quasi-native internal volume. However, the β-sheet region, containing the residues interacting with the channel is slightly distorted at the C-terminus and the N-terminal segment 1−3, containing the functional important residues pyroglutamic-1 and phenylalanine-2, is less well-defined and, apparently, more flexible than in the native toxin (*62*). Thus, even limited structural perturbations produce readily measurable effects on the channel blockage activity. This reveals a great sensitivity of the channel function on structural alterations of the toxin and emphasizes the intimate interaction between the functional molecular surface of the toxin and the outer channel binding surface (*12*).

Chab I presents a biological activity which is 180-fold reduced. This difference is the result of both a decrease in the association rate and an increase in the dissociation rate. This fact would suggest that the molecule suffers of structural perturbations larger than those observed in Chab II. However, in the case of the [7−37]charybdotoxin analogue (*47*), lacking the entire 1−6 segment, a K_D of 2.2×10^{-6} M for the same K^+ channel was determined (unpublished result); this implies a 260-fold reduction in affinity for the channel; 2D-NMR analysis of this analogue showed that the molecule retains the native secondary and tertiary structure (*47*). Furthermore, the fact that a core peptide (*63*), derived by the scorpion Leiurotoxin I, lacking the disulfide 3−21 (equivalent to the disulfide 7−28 of charybdotoxin) and truncated at the N-terminus, still maintains the secondary structure and the morphology of the α/β scorpion fold, may help to interpret the loss of activity of Chab I. These results suggest that the deletion of the disulfide bond 7−28 of charybdotoxin leaves the helix region intact, but affects the structure of the β-sheet and especially of the N-terminal region, which, longer in charybdotoxin than in Leiurotoxin I, may be much more flexible in Chab I and not any more aligned with the other strands to form the flat β-sheet surface described to interact with the channel. The altered near-UV CD spectrum which suggests a less fixed environment about the Tyr-36 in the β-sheet, is in agreement with this conclusion. Chab III, which lacks the disulfide 17−35, presents a decrease in biological potency of almost 3 orders of magnitude, which, as for Chab I, results from an increase in the dissociation rate and from a decrease in the association rate. Most probably, this molecule may present structural perturbations larger than those suggested for Chab I.

In summary, removal of the "central" disulfide bond 13−33 (see Figure 1A) minimally perturbs the structure of the toxin and only slightly affects the biological activity; removal of the "peripheral" disulfide 7−28 and 17−35 decreases the structural nativelikeness and the biological potency to a major extent, the last disulfide being the most sensitive. Thus, the functional consequence of removing one disulfide bond in charybdotoxin shows a marked dependence on the position of the bond implicated.

Studies on disulfide bridge deletion and engineering demonstrate that a disulfide contributes the most to protein structure and stability when it links large loops or connects N- and C-terminal lobes of the molecule, or is located within flexible regions (*64*). As shown in Figure 1, the disulfide 13−33 links the third β-strand to the helix. Its removal (as in Chab II), per se, should contribute a low entropic effect, since this bridge joins residues of the molecule that are already brought in proximity by the other two disulfides and it is present in a structurally well-defined region. In contrast, deletion of the bridges 7−28, as in Chab I, and of the bridge 17−35, as in Chab III, may have a much larger entropic effect, since these two bonds join residues that are closer to the N- and C-termini: removal of these covalent bonds are expected to free the ends of the polypeptide and to introduce an increased flexibility in regions already more exposed to the solvent.

Folding in Native and Denaturing Conditions. In the presence of glutathione, mature charybdotoxin is able to form the native disulfides with high yield and in a short time (*47*, *65*). Our studies on disulfide formation on the three Chab molecules reveal that the deletion of a pair of cysteines of the charybdotoxin sequence (and the substitution with two Aba residues) affects the pairing among the remaining cysteine residues differently, depending on the cysteine residues removed. As shown in Figure 6, among the four cysteines of each Chab sequence, three different pairings are possible, corresponding to three possible isomers: *globule*, *ribbon*, and *beads* (*43*).

From HPLC monitoring and ES-MS analysis of all the species formed after folding (in the absence of denaturant) (see Figure 5, top), it is evident that the absence of the disulfide 13−33 (as in Chab II) and 17−35 (as in Chab III) significantly reduces the capability of the remaining cysteines to find their right partner. This clearly suggests that these two disulfide bonds play a key role in the folding of charybdotoxin. The presence of the denaturant guanidine·HCl is a second factor influencing the pairing of the cysteine residues. In fact, while in the absence of denaturant the Chab II and Chab III sequences form all three possible isomers, in its presence the native isomer does not form any more and only the two nonnative *ribbon* and *beads* isomers are observed. Although the mechanisms by which guanidine·HCl acts are not fully understood, it is generally accepted that it weakens the hydrophobic interactions, thus decreasing the tendency of nonpolar groups to be buried in the folded conformation. The observed denaturant effects, thus, suggest that hydrophobic interactions are important in directing the folding of the Chab II and Chab III analogues and in stabilizing their structures. In fact, the structure of Chab II, as revealed by NMR analysis, is largely stabilized by hydrophobic interactions involving, in particular, the two Aba residues (*62*). The formation of Chab I seems to be much less sensitive to the presence of guanidine·HCl and the effect of addition of denaturant is to allow the formation of the *globule* and the nonnative *ribbon* isomers in equal proportion.

Recently, Sabatier et al. (*66*) synthesized three analogues of the scorpion toxin Leirotoxin I, lacking one disulfide, equivalent to the Chab analogues. At variance with the Chab derivatives, the only Leiurotoxin I analogue that formed with the native *globule* disulfide arrangement was the isomer lacking the disulfide 3−21, homologous to Chab I, while the other two presented the nonnative arrangements. However, in that study, 1 M guanidine·HCl was employed during folding: the utilization of the denaturant may explain the

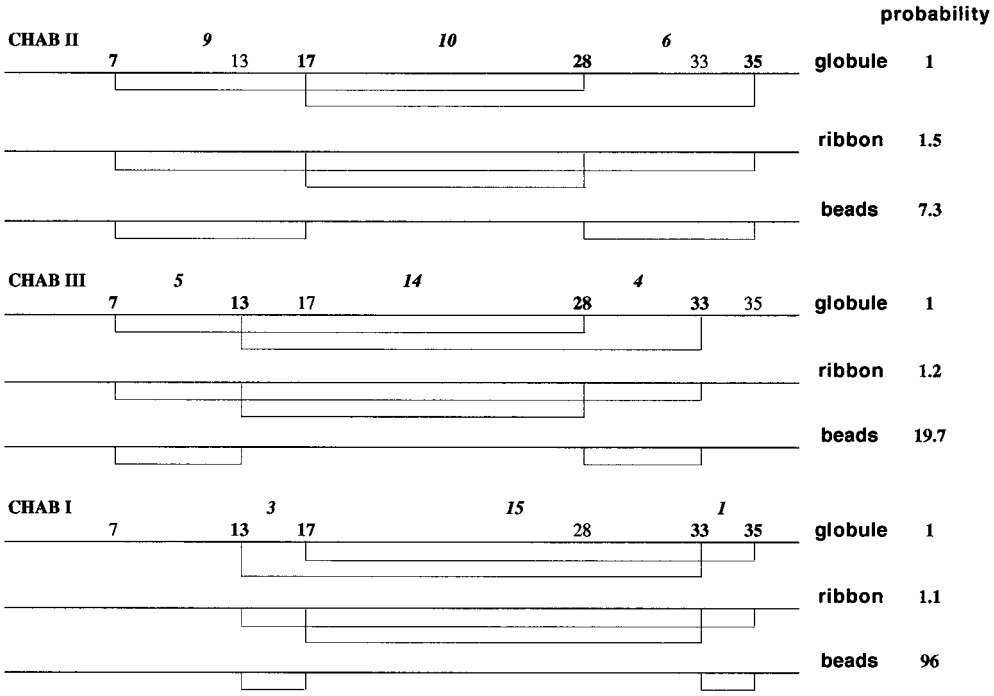

FIGURE 6: Possible isomers of Chab I, Chab II, and Chab III, corresponding to the three different pairings among the four cysteine residues of each analogue. Numbers in italics indicate the spacings between cysteines. Probabilities of formation of the different isomers have been calculated according to Kauzmann (*67*).

formation of nonnative bridges. Thus, in contrast to what reported in that paper, the presence of nonnative isomers is not unexpected. In particular, the HPLC profiles of the oxidation mixtures that were reported by Sabatier et al. (*66*) are rather similar to our HPLC profiles of the oxidation solutions in 6M guanidine.HCl (Figure 5, bottom).

Role of Cysteine Spacings. From probability calculations (*67*) on the possible disulfide arrangements of the three Chab sequences, we found that the *globule* isomer is always the least favored and the *beads* isomer is the most favored one (Figure 6). In particular, in the case of Chab I, the *beads* isomer is 96-fold more probable than any other isomer. However, this isomer does not form and only the native *globule* and the nonnative *ribbon* isomers are formed. This suggests that configurational entropy is playing a little role in the disulfide formation of charybdotoxin (vide infra).

From studies on model peptides, Snyder (*41*) and Zhang and Snyder (*42, 43*) showed that, for short peptide loops containing one or three residues separating two cysteines, the formation of a disulfide bond between the two cysteine residues implies a highly constrained conformation of the loop, and for this reason, it is thermodynamically disfavored. The *beads* isomer of Chab I would present these particular unfavorable spacings. We suggest that this is the reason, in Chab I folding, the *beads* isomer, although favored by probability considerations, never forms. Similarly, in the folding of apamin and endothelin, both containing spacings between cysteines similar to that of Chab I, the *beads* isomers have never been observed (*43*). Thus, it appears that a particular spacing between the cysteine residues is able by itself to prevent certain cysteine pairings and favor others. In the folding of Chab I, this will reduce the number of possible folding intermediates to only two, corresponding to the two favored cysteine pairings; specific noncovalent interactions, then, may preferentially stabilize the native *globule* arrangement. The presence of high concentration of denaturant appears to abolish the weak noncovalent interactions that allow discrimination between the two pathways, leading to the formation of both the native *globule* and the nonnative *ribbon* isomer. This proposed pathway of folding for Chab I is yet entirely hypothetical, but it provides a reasonable explanation for the high yield in formation of the native Chab I isomer. Given the high rate and high efficiency of the folding of native charybdotoxin, it is tempting to suggest that a pathway, implying the early and cooperative formation of the two disulfides 13−33 and 17−35 (thus leading to a Chab I type of intermediate), may be operative for native charybdotoxin. This hypothesis is being currently tested in our laboratory.

In the charybdotoxin structure (*22, 23*), the particular spacing of three residues between the two half-cystines of the helix and of one residue between those of the third β-strand have been proposed to be the structural consequence for joining the helix to the β-sheet by two disulfides: with those spacings the two side chains of the cysteines in the helix would be properly aligned with those in the β-strand, to form the disulfide bonds. The resulting sequence motif, C...CxxxC...C...CxC, has been recognized as the sequence consensus motif characterizing the α/β scorpion fold (*22, 23*). However, the structural and functional characterization of the Chab analogues clearly indicates that two evolutionary conserved cysteine residues of the consensus motif can be removed and yet the native fold be obtained (but with a lower yield). Therefore, conservation of the sequence motif, C...CxxxC...C...CxC, seems not to be an absolute requirement of the α/β scorpion structural motif. However, the spacings CxxxC and CxC appear to play a fundamental role in the folding process: its preservation allows efficient folding of Chab I and charybdotoxin, while its absence significantly compromises this ability (as in Chab II and Chab III). The

folding behavior of the corresponding analogues (lacking the disulfide 3−21) of the scorpion Leiurotoxin I (*66*) confirms this interpretation and suggests that it may apply to all scorpion toxins.

Implications for Protein Engineering. The α/β scorpion scaffold is a fold highly suggestive for protein engineering: its ability to yield, within a constant structure and a short sequence, a variety of functions (*68*) has already stimulated the design of original and artificial miniproteins presenting new functions (*31*, *32*). The results reported in this work, by contributing an increased knowledge on some basic rules that underlie the folding properties of the scorpion toxin and some relationships that link the structure to a particular cysteine spacing, may provide a more rational exploitation of the scorpion scaffold in the engineering of new functions. Furthermore, the present work provides the basis for an intervention even on some evolutionary conserved residues (the cysteines) in order to introduce new structural properties into the designed molecules. For example, the incorporation of two nonbridging Aba residues in the place of particular cysteine residues can now be planned in order to introduce a wanted conformational flexibility in specific structural regions of the α/β plateform. The possibility to rationally manipulate a very stable and versatile structural scaffold and to modulate more subtle structural properties, such as local conformational flexibility, may considerably augment the potentiality of the design by adding a better adaptation and an improved complementarity of the newly engineered molecules to their biological targets.

These conclusions are by no means limited to the scorpion scaffold, but may apply to other disulfide rich structures or domains. The (re)discovered role of cysteine spacings in governing specific disulfide arrangements may open new possibilities in the design of novel miniglobular structures that are stabilized by multiple disulfide bonds and are able to fold efficiently.

SUPPORTING INFORMATION AVAILABLE

Table 1. Peptide mapping of the purified analogue Chab I, Chab II, and Chab III (1 page). Ordering information is given on any current masthead page.

REFERENCES

1. Miller, C., Moczydlowski, E., LaTorre, R., and Phillips, M. (1985) *Nature 313*, 316−318.
2. Gimenez-Gallego, G., Navia, M. A., Reuben, J. P., Katz, G. M., Kaczorowski, G. J., and Garcia, M. L. (1988) *Proc. Natl. Acad. Sci. U.S.A. 85*, 3329−3333.
3. Guggino, S. E., Guggino, W. B., Green, N., and Saktor, B. (1987) *Am. J. Physiol. 252*, C128−C137.
4. Lewis, R. S., and Cahalan, M. D. (1988) *Science 239*, 771−775.
5. MacKinnon, R., and Miller, C. (1988) *Science 245*, 1382−1385.
6. Sands, S. B., Lewis, R. S., and Cahalan, M. D. (1989) *J. Gen. Physiol. 93*, 1061−1074.
7. Price, M., Lee, S. C., and Deutsch, C. (1989) *Proc. Natl. Acad. Sci. U.S.A. 86*, 10171−10175.
8. Schweitz, H., Stansfeld, C. E., Bidard, J. N., Fagni, L., Maes, P., and Lasdunski, M. (1989) *FEBS Lett. 250*, 519−522.
9. Vazquez, J., Feigenbaum, P., King, V. F., Kaczorowski, G. J., and Garcia, M. (1990) *J. Biol. Chem. 265*, 15564−15571.
10. MacKinnon, R., Heginbotham, L., and Abramson, J. (1990) *Neuron 5*, 767−771.
11. Goldstein, S. A. N., Pheasant, D. J., and Miller, C. (1994) *Neuron 12*, 1377−1388.
12. Stampe, P., Kolmakova-Partensky, L., and Miller, C. (1994) *Biochemistry 33*, 443−450.
13. Stocker, M., and Miller, C. (1994) *Proc. Natl. Acad. Sci. U.S.A. 91*, 9509−9513.
14. Hidalgo, P., and MacKinnon, R. (1995) *Science 268*, 307−310.
15. Aiyar, J., Withka, J. M., Rizzi, J. P., Singleton, D. H., Andrews, G. C., Lin, W., Boyd, J., Hanson, D. C., Simon, M., Dethlefs, B., Lee, C. L., Hall, J. E., Gutman, G. A., and Chandy, K. G. (1995) *Neuron 15*, 1169−1181.
16. Gross, A., and MacKinnon, R. (1996) *Neuron 16*, 399−406.
17. Naranjo, D., and Miller, C. (1996) *Neuron 16*, 123−130.
18. MacKinnon, R. (1991) *Nature 350*, 232−235.
19. MacKinnon, R., Aldrich, R. W., and Lee, A. W. (1993) *Science 262*, 757−759.
20. Robitaille, R., Garcia, M., Kaczorowski, G. J., and Charlton, M. P. (1993) *Neuron 11*, 645−655.
21. Reger, W. G., and Mintz, I. M. (1994) *Neuron 12*, 605−613.
22. Bontems, F., Roumestand, C., Boyot, P., Gilquin, B., Doljanski, Y., Ménez, A., and Toma, F. (1991) *Eur. J. Biochem. 196*, 19−28.
23. Bontems, F., Roumestand, C., Gilquin, B., Ménez, A., and Toma, F. (1991) *Science 254*, 1521−1523.
24. Johnson, B. A., and Sugg, E. E. (1992) *Biochemistry 31*, 8151−8159.
25. Johnson, B. A., Stevens, S. P., and Williamson, J. M. (1994) *Biochemistry 33*, 15061−15070.
26. Fernandez, L., Romi, R., Szendeffy, S., Martin-Euaclaire, M. F., Rochat, H., Van Rietschoten, J., Pons, M., and Giralt, E. (1994) *Biochemistry 33*, 14256−14263.
27. Krezel, A., Kasibhatla, C., Hidalgo, P., MacKinnon, R., and Wagner, G. (1995) *Protein Sci. 4*, 1478−1489.
28. Dauplais, M., Gilquin, B., Possani, L. D., Gurrola-Briones, Roumestand, C., and Ménez, A. (1995) *Biochemistry 34*, 16563−16573
29. Bonmatin, J.-M., Bonnat, J.-L., Gallet, X., Vovelle, F., Ptak, M., Reichhart, J.-M., Hoffmann, J. A., Keppi, E., Legrain, M., and Achstetter, T. (1992) *J. Biomol. NMR 2*, 235−256.
30. Bruix, Jiménez, M. A., Santoro, J., Golzales, C., Colilla, F. J., Méndes, E., and Rico, M. (1993) *Biochemistry 32*, 715−724.
31. Vita, C., Roumestand, C., Toma, F., and Ménez, A. (1995) *Proc. Natl. Acad. Sci. U.S.A. 92*, 6404−6408
32. Drakopoulou, E., Zinn-Justin, S., Guenneugues, M., Gilquin, B., Ménez A., and Vita, C. (1996) *J. Biol. Chem. 271*, 11974−11987.
33. Zinn-Justin, S., Guenneugues, M., Drakopoulou, E., Gilquin, B., Vita, C., and Ménez, A. (1996) *Biochemistry 35*, 8535−8543.
34. Creighton, T. E. (1990) *Biochem. J. 270*, 1−16.
35. Creighton, T. E. (1992) in *Protein Folding* (Creighton, T. E., Ed.) pp 301−351, W. H. Freeman, New York.
36. Weissman, J. S., and Kim, P. S. (1991) *Science 253*, 1386−1393.
37. Wearne, S. J., and Creighton. T. E. (1988) *Proteins: Struct., Funct., Genet. 4*, 251−261.
38. Rothwarf, D. M., and Scheraga, H. A. (1993) *Biochemistry 32*, 2671−2679.
39. Li, Y. J., Rothwarf, D. M., and Scheraga, H. A (1995) *Nat. Struct. Biol. 2*, 489−494.
40. Pace, C. N., and Creighton, T. E. (1986) *J. Mol. Biol. 188*, 477−486.
41. Snyder, G. H. (1987) *Biochemistry 26*, 688−694.
42. Zhang, R., and Snyder, G. H. (1989) *J. Biol. Chem. 264*, 18472−18479.
43. Zhang, R., and Snyder, G. H. (1991) *Biochemistry 30*, 11343−11348.
44. Ramalingam, K., and Snyder, G. H. (1993) *Biochemistry 32*, 11155−11161.

45. Wlodawer, A., Miller, M., Jaskolski, M., Sathyanarayana, B. K., Baldwin, E., Weber, I. T., Selk, L. M., Clawson, L., Schneider, J., and Kent, S. B. H. (1989) *Science 245*, 616−621.
46. Ferrer, M., Woodward, C., and Barany, G. (1992) *Int. J. Peptide Protein Res. 40*, 196−207.
47. Vita, C., Bontems, F., Bouet, F., Tauc, M., Poujeol, P., Vatanpour, H., Harvey, A. L., Ménez, A., and Toma, F. (1993) *Eur. J. Biochem. 217*, 157−169.
48. Vita, C., Bontems, F., Roumestand, C., Tauc, M., Poujeol, P., Ménez, A., and Toma, F. (1993) in *Peptides 1992* (Schneider, C. H., and Eberle, A. N. Eds.) pp 641−642, ESCOM.
49. Moczydlowski, E., and LaTorre, R. (1983) *Biochim. Biophys. Acta 732*, 412−420.
50. Fields, C. G., Lloyd, D. H., Macdonald, R. L., Otteson, K. M., and Noble, R. L. (1991) *Peptide Res. 4*, 95−101.
51. Grandas, A., Jorba, X., Giralt, E., and Pedroso, E. (1989) *Int. J. Peptide Protein Res. 33*, 386−390.
52. Sarin, V. K., Kent, S. B. H., Tam, J. P., and Merrifield, R. B. (1983) *J. Am. Chem. Soc. 105*, 6442−6455.
53. King, D. S., Fields, C. G., and Fields, G. B. (1990) *Int. J. Peptide Protein Res. 36*, 255−266.
54. Neyton, J., and Pelleschi, M. (1991) *J. Gen. Phys. 97*, 641−665.
55. Golowasch, J., Kirkwood, A., and Miller, C. (1986) *J. Exp. Biol. 124*, 5−13.
56. Hanke, W.; Miller. C. (1983) *J. Gen. Phys. 82*, 25−45.
57. Neyton, J., and Miller, C. (1988) *J. Gen. Phys. 92*, 549−567.
58. Anderson, C. S., MacKinnon, R., Smith, C., and Miller, C. (1988) *J. Gen. Phys. 91*, 317−333.
59. Sakakibara, S. (1995) *Biopolymers (Peptide Sci.) 37*, 17−28.
60. Park, C. S., and Miller, C. (1992) *Neuron 9*, 307−313.
61. Park, C. S., and Miller, C. (1992) *Biochemistry 31*, 7749−7755.
62. Song, J., Gilquin, B., Jamin, N., Drakopoulou, N., Guenneugues, M., Dauplais, M., Vita, C., and Ménez, A. (1997) *Biochemistry 36*, 3760−3766.
63. Pagel, M. D., and Wemmer, D. E. (1994) *Proteins 18*, 205−215.
64. Matsumura, M., Becktel, W. J., Levitt, M., and Matthews, B. W. (1989) *Proc. Natl. Acad. Sci. U.S.A. 86*, 6562−6566.
65. Lambert, P., Kuroda, H., Chino, N., Watanabe, T. X., Kimura, T., and Sakakibara, S. (1990) *Biochem. Biophys. Res. Commun. 170*, 684−690.
66. Sabatier, J. M., Lecomte, C., Mabrouk, K., Darbon, H., Oughideni, R., Canarelli, S., Rochat, H., Martin-Eauclaire, M. F., and Van Rieschoten, J. (1996) *Biochemistry 35*, 10641−10647.
67. Kauzmann, W. (1959) in *Sulfur in Proteins* (Benesch, R., Benesch, R. E., Boyer, P. D., Klotz, I. M., Middlebrook, W. R., Szent-Gyorgyi, A. G., and Schwarz, R. D., Eds.) pp 93−108, Academic Press, New York.
68. Ménez, A., Bontems, F., Roumestand, C., Gilquin, B., and Toma, F. (1992) *Proc. R. Soc. Edinburgh 99*B, 83−103.
69. Galvez, A., Gimenez-Gallego, G., Reuben, J. P., Roy-Contancin, L., Feigenbaum, P., Kaczorowski, G. J., and Garcia, M. L. (1990) *J. Biol. Chem.* 265, 11083−11090.
70. Garcia-Calvo, M., Leonard, R. J., Novick, J., Stevens, S. P., Schmalhofer, W., Kaczorowski, G. J., and Garcia, M. L. (1993) *J. Biol. Chem. 268*, 18866−18874.
71. Possani, L. D., Martin, B. M., and Svevdensen, J. (1982) *Carlsberg Res Commun. 47*, 285−289.
72. Crest, M., Jacquet, G., Gola, M., Zerrouk, H., Benslimane, A., Rochat, H., Mansuelle, P., and Martin-Eauclaire, M. F. (1992) *J. Biol. Chem. 267*, 1640−1647.
73. Garcia, M. L., Garcia-Calvo, M., Hidalgo, P., Lee, A., and MacKinnon, R. (1994) *Biochemistry 33*, 6834−6839.
74. Rogowski, R. S., Krueger, B. K., Collins, J. H., and Blaustein, M. P. (1994) *Proc. Natl. Acad. Sci. U.S.A. 91*, 1475−1479.
75. Chicchi, G. G., Gimenez-Gallego, G., Ber, E., Garcia, M. L., Winquist, R., and Cscieri, M. A. (1988) *J. Biol. Chem. 263*, 10192−10197.
76. Zerrouk, H., Mansuelle, P., Benslimane, A., Rochat, H., and Martin-Eauclaire, M. F. (1993) *FEBS Lett. 320*, 189−192.
77. Blanc, E., Fremont, V., Sizun, P., Meunier, S., Van Rietschoten, J., Thevand, A., Bernassau, J. M., and Darbon, H. (1996) *Proteins: Struct., Funct., Genet. 24*, 359−369.

BI9721086